

Research Paper: Investigation of Organ Dose in Dental CBCT Using GATE Monte-Carlo Code



Arezoo Jafarian¹ , Sedigheh Sina^{1,2} * , Rasool Safari¹

¹Nuclear engineering department, Shiraz University, Shiraz, Iran

²Radiation Research Center, Shiraz University, Shiraz, Iran

Use your device to scan
and read the article online



Citation: Jafarian A, Sina S, Safari R. Investigation of Organ Dose in Dental CBCT Using GATE Monte- Carlo Code. Journal of Dentomaxillofacial Radiology, Pathology and Surgery. 2020; 9(1):12-17. <http://dx.doi.org/10.32598/3dj.7.4.145>

<http://3dj.gums.ac.ir>



Article info:

Received: 2020/01/28

Accepted: 2020/02/29

Keywords:

Phantoms, Imaging Radiometry , Spiral Cone-Beam Computed Tomography

ABSTRACT

Introduction: Patient dose is the most important concern for any new X-ray system. The dose received by the patients depends on the imaging technique, the optimization of the collimator, filtration and field of view (FOV). The purpose of this study is to evaluate the effect of various imaging parameters on dose received by different organs in a dental CBCT scanners.

Materials and Methods: In this study, dental CBCT system (Planmeca 3d mid) including the X-ray tube, flat panel detector and a voxelized phantom, was simulated by the GATE Monte-Carlo Code (Version 8). DICOM CBCT images of a person, and Alderson Rando phantom were segmented using MATLAB and 3D slicer software to identify various organs such as bone, bone marrow, soft tissue, brain and thyroid.

Results: The half value layer of the simulated X-ray was found to be 2.6 mm which differed from the experimental value by approximately 6.47%. In some cases, the 3D dose distribution for Rando Phantom was less than that for Voxelized phantom simulated by CT images of a normal person.

Conclusion: The reason of this difference is attributed to the different substances definition. The difference in experimental and simulation data can be due to several reasons i.e. the inaccuracy caused by the use of a limited number of TLDs in experimental measurements, the impossibility of simulating Gentry's actual rotation (hyperbolic's rotation) and the uncertainties caused by converting CT images to e Voxelized phantom.

* Corresponding Author:

Sedigheh Sinai.

Address: Nuclear engineering department,
Shiraz University, Shiraz, Iran.

Tel: +98 (13) 33330862

E-mail: sina@gmail.com

Introduction

Cone-beam computed tomography (CBCT) technology was introduced in 1996 in Europe and in 2001 in the United States, and was a great step forward in dental imaging. In addition to dental imaging, CBCT systems are used in angiography imaging and Mega-Voltage radiotherapy. CBCT has two main hardware differences compared to CT; first, the CBCT uses fixed anode with low output. Second, CBCT devices rotate around the patient only once and collect the data using cone-shaped beams. As usual, the important concern for any new X-ray system is the patient dose, which is dependent on mAs and kV_p , as well as optimization of the collimator and filtration and field of view (FOV)(1).

As briefly mentioned, the CT technology has advanced in the direction of widening the beam width; this created the capability of acquiring a larger imaging area with fewer numbers of scans, while reducing the scan duration. Despite all the benefits of the wide beam CT system, this wide beam geometry introduced the difficulty of patient dosimetry because the conventional CTDI concept is not directly applicable to the cone beam CT (CBCT) geometry for the purpose of accurate radiation dose estimation in the phantoms. The reason is that the ionization created by a wide cone beam cannot be completely collected without any loss by a conventional CT pencil ion chamber; the wide cone beam creates a longer CT profile (approximately 30-100 cm). This makes it difficult for the current pencil ion chamber to physically cover the entire length. Even if one could create such a long pencil ion chamber, there would be many technical problems such as electron collection efficiency, electric field inhomogeneity, charged particle equilibrium, and so forth. Additionally, longer CT phantoms would also be needed for the measurements. To overcome these limitations, Thermoluminescence dosimetry is widely used for estimation of organ dose in CBCT, However this method has also a limitation which is the limited number of TLDs in each organ. Therefore Monte Carlo (MC) technique can be

used for the accurate CBCT dosimetry (2). The purpose of this study is to investigate the dose to different organs in CBCT, using Gate Monte Carlo code, by simulating voxelized phantoms.

Materials and Methods

In this section, dental CBCT system (Planme-ca 3d mid) includes the X-ray tube, flat panel detector and Voxelized phantoms, i.e. a normal person and Rando phantom, was simulated by the GATE Monte-Carlo Code (Version 8). The physical components of this system are obtained using the manual (materials used in the construction of the tube, the size, dimensions and geometric arrangement of different parts and, etc.) (3).

Monte Carlo Simulations:

The free Monte Carlo simulation code, Gate (version 8), is a simple, and convenient user interface of GEANT, facilitating the use of GEANT capabilities. Its prominent capabilities include the ability to:

- simulate CT, SPECT, PET and optical imaging systems,
- simulate electric, or magnetic fields,
- simulate movement and time-dependent concepts;
- Create Voxelized phantoms from CT, PET, and SPECT images.

Gate Monte Carlo code has been widely used in radiotherapy dose calculations.(4)

Simulation of a dental CBCT scanner:

The simulation consists of a tungsten anode, and a target with dimensions of $0.5 \times 0.5 \text{ mm}^2$, and the angle of 5 degrees relative to the vertical line, embedded in a glass cubical shell with the internal dimension of $12 \times 1 \times 1 \text{ cm}^3$, and the thickness 2mm. The source was defined as a mono-energetic electron beam. The dimensions, thickness and the distance of the anode of aluminum filter, were considered to be $80 \times 80 \text{ cm}$, 0.25cm, and 4cm respectively. Such values were $80 \times 80 \text{ cm}$, 0.05cm, and 4.025cm,

for copper Filter. To create a fan beam and limit the output beam on the detector a lead collimator with a thickness of 7cm, an opening of $6.5 \times 6.5\text{cm}^2$ and $13 \times 11.05 \text{ cm}^2$ with an interval of 6cm from the anode were used. The geometric range of particles tracking cube was considered to $100 \times 100 \times 100\text{cm}^3$. Figure 1 shows tube body, filters and collimator.

To increase run speed of the simulation, the photon source replaces the X-ray tube. The photon source's energy distribution follows the X-ray spectrum and the number of photon beam is obtained from Formula 1.

$$F_{p1} = N_p / N_{e1}$$

In the formula 1, f_{p1} the fraction of photons passing after the collimator, N_p the number of photons passing after the collimator (using the phase space Actor output), N_{e1} is the number of electrons used in simulation (two billion).

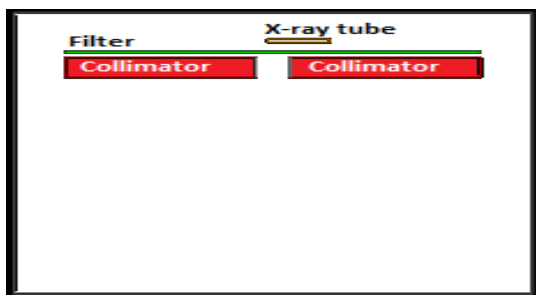


Figure 1: Simulated X-ray tube, filter, and collimator

Simulation of the Voxelized phantom

In this section, we used DICOM CBCT images of Alderson Rando phantom, and CBCT image set of a person for simulation of the equivalent human phantom using the GATE computational code.

Material type, and density of the constituent elements in the body of the simulated phantom, obtained based on the ICRU standard, are shown in Table 1. Voxelized phantom is located in the center of iso-center and Voxelized phantom rotates instead of the Photon source. For both NT and PM systems, the red, black, green, blue and purple lines, respectively, the field of view $8 \times 8\text{cm}^2$, $12 \times 8\text{cm}^2$, $15 \times 15 \text{ cm}^2$

Table 1. Texture composition in female alderson Rando Phantom(5)

ELEMENT	LUNG	MUSCLE	SKELETON
H	5.74	8.87	3.4
C	73.94	66.81	15.5
O	2.01	3.10	4.2
NA	-	-	0.1
MG	-	-	0.2
P	-	-	10.3
S	-	-	0.3
CA	-	-	22.5
SB	0.16	0.08	-
DENSITY (G/CM3)	0.32	1.00	1.92

Simulation detector

A flat panel detector with dimensions $14.6 \times 0.5 \times 14.6\text{cm}$ consists of three sub-layers: a $14.6 \times 0.5 \times 14.6\text{cm}$ module, $14.6 \times 0.5 \times 14.6\text{cm}$ a cluster and $0.1 \times 0.5 \times 0.1 \text{ cm}$ pixels as sensitive detector volume of silicone material. Figure 2 shows the detector and Voxelized phantom (a normal person and Rando-phantom).

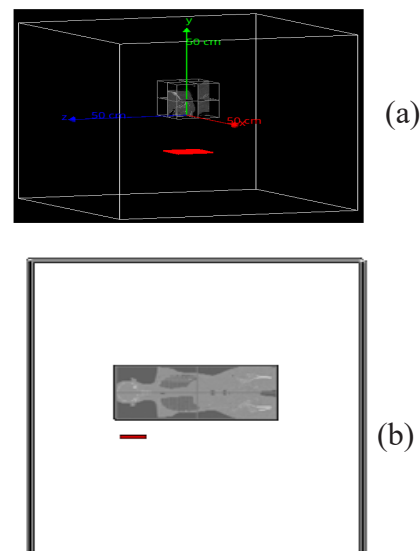


Figure 2: Schematic detector and Voxelized phantom (a) normal person (b) Rando phantom

Result

Extraction of the X-ray tube spectrum

The X-ray tube spectrum was extracted using the detector output (in text format) analyzed by the MATLAB R2014a software. Figure 3 shows the normalized spectrum extracted from the simulation.

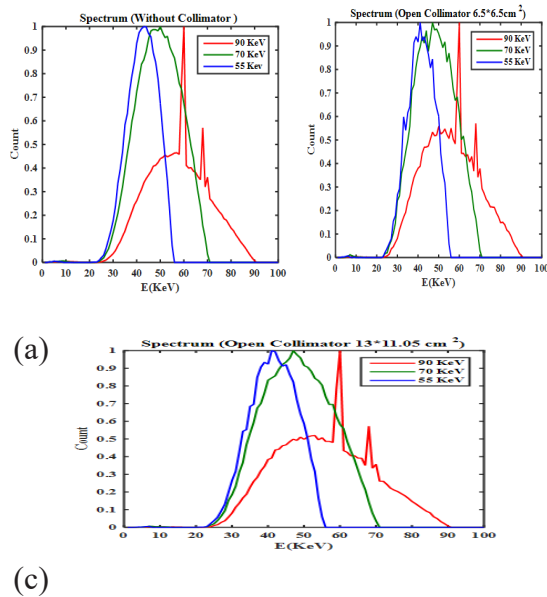


Figure 3: The normalized spectrum of the X-ray tube with total filtration (0.5mmAl + 0.25mm Cu) for energies 55, 70 and 90 keV a) without collimator b) collimator opening 6.5×6.5cm² (field of view 10×10cm²) (c) collimator opening 13×11.05cm² (field of view 20×17cm²).

Table 3. Comparison of HVL simulations with experimental results, and a previous work.

KVP	MA	Time (s)	FOV (cm ²)	HVL (mm AL) GATE	HVL (mm AL) quality control	HVL (mm AL) (7)
70	6	0.2	6*6	2.6	2.85	2.78
63	6	0.2	6*6	2.42	-	2.50
60	7	0.1	6*6	2.23	-	2.37

Extraction of 3D dose distribution:

3Dsliser and MATLAB R2014a software were used to segment the organs. The MATLAB R2014a software reads the output file for the Actor dose output, raw and mhd format, and extracts the 3D dose distribution.

The average dose for 14mA currents for Rando and normal person phantom are shown in Tables 4, and 5.

Once the dose to each organ is obtained, the equivalent dose HT is obtained by equation 2, and the effective dose is obtained by equation 2.

$$H_T = W_R \times \sum_i f_i \times D_{Ti}$$

Where WR is radiation weighting factor, fi is the mass fraction of the tissues

Validation of the simulations

For validation of the simulated X-ray tube, the tungsten Characteristic peak simulation was compared with the results of IPEM78 (Table 2).

Table 2. Comparison tungsten Characteristic peak simulation with IPEM78 for 90 keV energy

	IPEM78(6)	GATE
K _{A2} (KEV)	57.9817	58.2
K _{B1} (KEV)	67.2443	67.5
K _{A1} (KEV)	59.31824	59.5

Ti in the slice i that has been irradiated, and DTi is the average absorbed dose in the fraction of tissue/organ T contained in the slice i, as presented by Ghaedi et al.

$$E = \sum_T W_T H_T$$

Table 6 compares the experimental and simulation results of the effective dose.

Table 4: The results of the 3D dose distribution of organs (Rando phantom Voxelized) for 14mA, different voltages and FOVs

KV _p	FOV	mAs	Bone Marrow (GY)	BONE (GY)	SOFT (GY)	BRAIN (GY)
90	10*10	169	1.55E-04	2.099E-04	1.57E-04	1.027E-04

Table 5: The results of the 3D dose distribution of organs (normal person Voxelized phantom) for 14mA, different voltages and FOVs

KV _p	FOV	mAs	BONE MARROW(GY)	BONE (GY)	SOFT (GY)	BRAIN (GY)
55	10*10	169	2.7748E-05	3.9998E-05	2.8757E-05	1.7408E-05
70	10*10	169	7.7488E-05	1.0904E-04	7.8741E-05	4.9807E-05
90	10*10	169	1.9105E-04	2.6150E-04	1.9328E-04	1.2609E-04
55	20*17	380	5.4342E-05	7.0940E-05	5.4454e-05	3.6792E-05
70	20*17	380	1.5008e-04	1.9475E-04	1.4966e-04	1.048E-04
90	20*17	380	3.6717e-04	4.6823E-04	3.6706E-04	2.5512E-04

Table 6. Experimental and simulation results for dental CBCT system (Planmeca 3d mid)

	FOV (cm2)	kv _p	mas	Bone Marrow (μsv)	Bone (μsv)	BRAIN MSV))
Experimental data[8]	10*10	90	169	111.96	----	531
Simulation normal phantom	10*10	90	169	191.05	261.50	126.09
Simulation Rando phantom	10*10	90	169	154.39	208.65	102.14

Discussion and Conclusionns

GATE Monte Carlo code was used in this study for dosimetry in dental CBCT images. The simulations were performed for Rando phantom, and a normal person for different field of views, and kVps. As it is evident from the results, with constant field of view, the organ doses increase with increasing voltage. As the voltage increases, in addition to increasing the number of photons, the average energy increases, resulting in higher doses. With constant voltage, the organ doses increase with increasing field of view, because of increasing the irradiated volume, and scattered radiation.

The difference in dose to organs of Rando Phantom, and normal patient voxelized phantom is due to the different geometry, and density of tissues. The difference between the experimental and simulation data is mainly because of the inaccuracy caused by the use of a limited number of TLDs in experimental measurements. The impossibility of simulating Gentry's actual rotation (hyperbolic's rotation) and the uncertainties caused by converting CT images to e Voxelized phantom may be two other reasons for such a difference. However the main

reason is the limited number of dosimeters in the experimental work, as stated by Ghaedi et al, the number of TLDs for measurement of the brain dose is two, while in our simulation, all regions of brain is considered in the dose measurements.

It can be concluded that Monte Carlo codes are powerful tools in CBCT dosimetry, as we can overcome the limitations imposed in experimental measurements.

References

1. Palomo, J. M., Rao, P. S., & Hans, M. G. (2008). Influence of CBCT exposure conditions on radiation dose. *Oral Surgery, Oral Medicine, Oral Pathology, Oral Radiology, and Endodontology*, 105(6), 773-782. <https://doi.org/10.1016/j.tripleo.2007.12.019>
2. Kim, S. (2010). Cone Beam Computed Tomography (CBCT) Dosimetry : Measurements and Monte Carlo Simulations, (July). <https://doi.org/10.1097/HP.0b013e3181cd3ec3>
3. Hiltunen E., Niemi, M. (2012). Planmeca proMax 3D mid, technical manual, publication part number 10026634 rvision6, RELEASED.
4. Jan, S. et al. GATE: a simulation toolkit for PET and SPECT. *Phys. Med. Biol.* 49(19), 4543-4561 (2004).
5. Boia, L. S., Martins, M. C., Júnior, H. A. S., Silva,

- A. X., & Soares, A. F. N. S. (2011). Preparing a voxel-simulator of Alderson Rando physical phantom, 1-10.
6. Cranley K, Gilmore BJ, Fogarty GWA, Desponds L. IPEM Report 78: Catalogue of Diagnostic X-ray Spectra and Other Data (CD-Rom Edition 1997) (Electronic Version prepared by D Sutton) (York: The Institute of Physics and Engineering in Medicine (IPEM)) 1997.
7. Han, G., Cheng, J., Li, G., & Ma, X. (2013). Shielding effect of thyroid collar for digital panoramic radiography. <https://doi.org/10.1259/dmfr.20130265>
8. Ghaedizirgar, M., Faghihi, R., Paydar, R., Sina, S., Effective dose in two different dental CBCT systems; New Tom VGi and Planmeca 3D Mid, Radiation protection dosimetry, 2016. <https://doi.org/10.1093/rpd/ncx008>